resistivity does not continue increasing quadratically as predicted by the Wiedemann-Franz law and Eq. (13a). The field dependence of $\bar{\epsilon}_{yy}'$ (41) would be smaller than predicted from a ρ^2 dependence. This would reduce the theoretical amplitude predicted by Eq. (55).

The relatively good agreement between theory and experiment supports the use of Eq. (38) and the assumptions leading to it. It also shows that the Horton free-electron theory, and the assumption of randomly located neutral point impurities were reasonably good.

VI. SUMMARY

The adiabatic Nernst-Ettingshausen coefficient ϵ_{xy}', the thermoelectric coefficient ϵ_{yy}', and the thermal transverse-even coefficient ϵ_{zy}' are measured in magnetic fields to 3.3 T (33 kG) and temperatures between 1.2 and 4.2 K. The results clearly demonstrate the effects of Fermi-surface topology on ϵ_{xy}'.

The field and temperature dependence for the adiabatic coefficients are predicted by assuming the validity of the Wiedemann-Franz law and a theory for the isothermal coefficients. For closed-orbit directions, the field dependence of ϵ_{xy}' is AH^3+BH^2, in agreement with predictions. The coefficients ϵ_{yy}' and ϵ_{zy}' do not have observable (nonoscillatory) field dependencies. This is not in agreement with predictions. The coefficient ϵ_{xy}' is independent of temperature below 1.6°K, in agreement with predictions.

The adiabatic thermoelectric coefficient ϵ_{yy}' has strong quantum oscillations originating from the sixth-zone electron Fermi surface. The magnitude of these is in reasonably good agreement with the amplitude predicted by theory.

ACKNOWLEDGMENTS

The author wishes to express his thanks to Dr. D. J. Flood for helpful suggestions; and to Dr. P. A. Schroeder and Dr. J. Longo, especially for their assistance with parts of Sec. II B.

PHYSICAL REVIEW VOLUME 185, NUMBER 3 15 SEPTEMBER 1969

Lattice Dynamics of Beryllium Using a Pseudopotential Approach

V. C. SAHNI AND G. VENKATARAMAN
Nuclear Physics Division, Bhabha Atomic Research Centre, Trombay, Bombay-85, India
(Received 21 March 1969)

The lattice dynamics of Be is discussed within the framework of the local pseudopotential approximation. Calculations are made in the first instance using a basic pseudopotential computed from the orthogonalized-plane-wave band-structure results of Loucks and Cutler. Comparison with experimental phonon dispersion relations shows, however, poor agreement. Calculations are also made using Heine–Animalu model potentials, with similar results. Finally, the experimental data are inverted to obtain an experimental pseudopotential. The latter is used to make a band-structure calculation, and the resulting Fermi surface is compared with that derived from de Haas–van Alphen experiments.

I. INTRODUCTION

IN recent years, calculations of the phonon dispersion relations for a number of cubic metals have been reported using the pseudopotential approach. The method was first extended to hcp metals by Roy and Venkataraman,[1] and explicit calculations were made for Mg. Continuing this program, we present in this paper similar results for Be. As in the case of our work on Mg, calculations were made in the first instance from basic principles without any adjustable parameters, using as input information some results from the orthogonalized-plane-wave (OPW) band-structure work of Loucks and Cutler.[2] These calculations, when compared with the experimental results of Schmunk *et al.*[3] showed only qualitative agreement except for the transverse branches along the [0001] direction, where the agreement was good. Dispersion relations were then obtained using the results of Animalu[4] based on the Animalu-Heine model potential[5] which, it may be recalled, has been used with fair success in computing various electronic properties for a number of cubic metals. These also showed only qualitative agreement with experimental dispersion relations, the agreement being in fact worse than that obtained in the first-principles work. Calculations were also made using a model potential computed by Animalu[6] along the lines

[1] A. P. Roy and G. Venkataraman, Phys. Rev. **156**, 769 (1967). Unfortunately, the numerical results presented in this paper are in error owing to a mistake in the formula for the Coulomb contribution. Specifically, the expression for the Coulomb contribution from atoms in the same sublattice given in Eq. (7) of this paper is valid only for cubic symmetry. Equation (8), which gives the contribution from different sublattices is, however, valid for all symmetries. The mistake in Eq. (7) was subsequently rectified and the proper numerical results presented in an addendum (unpublished).

[2] T. L. Loucks and P. H. Cutler, Phys. Rev. **133**, A819 (1964).

[3] R. E. Schmunk, R. M. Brugger, P. D. Randolph, and K. A. Strong, Phys. Rev. **128**, 562 (1962).

[4] A. O. E. Animalu, Proc. Roy. Soc. (London) **A294**, 376 (1966).

[5] A. O. E. Animalu and V. Heine, Phil. Mag. **12**, 1249 (1965).

[6] A. O. E. Animalu (private communication). We are grateful to Dr. Animalu for making available to us these unpublished results.

recently employed by Animalu *et al.*[7] in connection with their work on phonon spectra of cubic metals, and these too were found to be inadequate. Finally, we have inverted the experimental phonon data to obtain an "experimental pseudopotential" so as to provide a basis for computing the various properties of Be. This was in the same spirit as a similar program undertaken successfully by Stoll and Schneider[8] for Mg. By way of assessing the usefulness of our fitted potential, we have carried out a band-structure calculation. A noteworthy feature of this band structure is that it is more nearly free-electron-like than those obtained from OPW[2] and (augmented plane wave) (APW)[9] calculations. In passing we might remark that the basic and model potentials also yield nearly free-electron-like band structures. We have also computed representative dimensions of the Fermi surface using the experimental pseudopotential and these have been compared with those obtained from de Haas–van Alphen experiments.[10] The results of the various calculations are presented in the following sections.

II. BASIC CALCULATIONS

The pseudopotential approach to lattice dynamics has been adequately discussed in the literature,[11] and does not warrant any repetition here. It is sufficient to recall for our purposes that in this formalism, the vibrational energy is made up essentially of three parts. The first of these is due to Coulomb interaction of positive ions immersed in a uniform compensating background of electrons, and the corresponding contributions to the elements of the dynamical matrix may be evaluated using standard methods.[12,13] The second contribution to the vibrational energy arises from ion core repulsions and is negligible in the case of Be since the size of the core is very much smaller than the nearest-neighbor distance.[14] The final contribution to the energy is associated with the response of the electrons to ionic motions. For a lattice with a basis the corresponding contributions to the dynamical matrix are given by[15]

$$D_{\alpha\beta}{}^{E}(\mathbf{q},kk)=\frac{2Z}{nM}\sum_{\tau}[(\tau+\mathbf{q})_{\alpha}(\tau+\mathbf{q})_{\beta}E(|\tau+\mathbf{q}|)-(\tau)_{\alpha}(\tau)_{\beta}F(k)E(|\tau|)], \quad (1)$$

$$D_{\alpha\beta}{}^{E}(\mathbf{q},kk')=\frac{2Z}{nM}\sum_{\tau}(\tau+\mathbf{q})_{\alpha}(\tau+\mathbf{q})_{\beta}E(|\tau+\mathbf{q}|)\times e^{-i\tau\cdot\mathbf{r}(k'k)}. \quad (2)$$

In the above equations, n is the number of ions in the primitive cell ($=2$ for Be), Z is the valency ($=2$ for Be), and M the mass of the ion (the crystal is assumed to be monatomic). Further, τ is a reciprocal-lattice vector and

$$\mathbf{r}(k'k)=\mathbf{r}(k')-\mathbf{r}(k),$$

where $\mathbf{r}(k)$ and $\mathbf{r}(k')$ denote, respectively, the equilibrium positions of the k and k'th ions in the primitive cell. The quantity $F(k)$ is given by

$$F(k)=\sum_{k'}\cos[\tau\cdot\mathbf{r}(k'k)].$$

The function $E(q)$ contains all the information about the electron behavior in the crystal, and in the local pseudopotential approximation is given by[16]

$$E(q)=-\tfrac{1}{2}[U(q)]^{2}\chi(q)/\epsilon(q), \quad (3)$$

where $U(q)$ is the Fourier transform of the bare local pseudopotential and

$$\chi(q)=\frac{3}{2E_F}\left(\frac{1}{2}+\frac{4k_F{}^{2}-q^{2}}{8k_Fq}\ln\left|\frac{q+2k_F}{q-2k_F}\right|\right), \quad (4)$$

k_F and E_F being the free-electron Fermi wave vector and Fermi energy, respectively. $\epsilon(q)$ is the wave-number-dependent dielectric function of the electron gas for which several expressions have been proposed. In the present paper we have adopted the following formula:

$$\epsilon(q)=1+\frac{4\pi Ze^{2}}{q^{2}\Omega_0}\chi(q)\left(1-\frac{q^{2}}{2(q^{2}+k_F{}^{2}+k_s{}^{2})}\right) \quad (5)$$

given by Sham,[17] which takes account of exchange effects. The quantities k_s and Ω_0 in Eq. (5) denote the screening length and atomic volume, respectively. The values of the various parameters for Be are listed in Table I.

The crux of the problem is to compute $U(q)$ and this was done in the present work using recently obtained band-structure results,[2] and the methods previously

TABLE I. Crystallographic and relevant parameters for Be.[a]

Unit cell constants	a	4.3211 a.u. (2.286 Å)
	c	6.7715 a.u. (3.583 Å)
	c/a	1.5671
Atomic volume		54.750 (a.u.)^3
Free-electron Fermi momentum	k_F	1.027 (a.u.)$^{-1}$
Thomas–Fermi screening length	k_s	1.1137 k_F
Mass of the ion	M	1.4958×10^{-23} g
Charge on the ion	$Z\|e\|$	2.0 $\|e\|$
Free-electron Fermi energy	E_F	1.0537 Ry
Atomic core energy level	E_{1s}	−6.765 Ry

[a] Taken from Ref. 2.

[7] A. O. E. Animalu, F. Bonsignori, and V. Bortolani, Nuovo Cimento **44**, 159 (1966).
[8] E. Stoll and T. Schneider, Physik Kondensierten Materie **8**, 58 (1968).
[9] J. H. Terrel, Phys. Rev. **149**, 526 (1966).
[10] B. R. Watts, Phys. Letters **3**, 284 (1963); Proc. Roy. Soc. (London) **A282**, 521 (1964).
[11] S. K. Joshi and A. K. Rajagopal, in *Solid State Physics*, edited by F. Seitz and D. Turnbull (Academic Press Inc., New York, 1968), Vol. 22, p. 159.
[12] E. W. Kellermann, Phil. Trans. Roy. Soc. (London) **A238**, 513 (1940).
[13] In addition to the addendum mentioned in Ref. 1, the correct version of Eq. (7) of the paper of Roy and Venkataraman may be found in Ref. 8.
[14] C. Herring and A. G. Hill, Phys. Rev. **58**, 132 (1940).
[15] Note that the equations given here differ slightly from Eqs. (13) and (14) of Ref. 1. We have exploited the inversion symmetry of the reciprocal lattice and avoided writing here the terms involving $(\tau-\mathbf{q})$.
[16] W. A. Harrison, *Pseudopotentials in the Theory of Metals* (W. A. Benjamin, Inc., New York, 1966).
[17] L. J. Sham, Proc. Roy. Soc. (London) **A283**, 33 (1965).

employed by Sham for his calculations on Na, i.e., in his model A.[17,18] The details are described below.

We observe, first of all, that the pseudopotential is really nonlocal and is, to some extent, arbitrary, as pointed out by Cohen and Heine.[19] A convenient form for the pseudopotential operator due to Austin *et al.*[20] is

$$U(\mathbf{r},\mathbf{r}',\mathbf{R})=U_b(\mathbf{r}-\mathbf{R})+\sum_t|\phi_t(\mathbf{r}-\mathbf{R})\rangle \times\langle\phi_t(\mathbf{r}'-\mathbf{R})|\,(T-E_t)$$
$$=U_b(\mathbf{r}-\mathbf{R})+U_R(\mathbf{r},\mathbf{r}',\mathbf{R}).$$

Here $U(\mathbf{r},\mathbf{r}',\mathbf{R})$ is the nonlocal pseudopotential operator associated with an ion at $\mathbf{R}$. $U_b(\mathbf{r}-\mathbf{R})$ is the bare potential of the ion and is local, while $U_R(\mathbf{r},\mathbf{r}',\mathbf{R})$ is the nonlocal operator associated with the repulsive part of the potential and depends on the core eigenfunctions $|\phi_t\rangle$ and the core eigenvalues E_t. T is the kinetic energy operator.

What is required in the present calculations is

$$U(q)=U_b(q)+\bar{U}_R(q),$$

where $U_b(q)$ is the Fourier transform of $U_b(r)$, and $\bar{U}_R(q)$ is a suitably averaged local repulsive potential.

Let us consider the calculation of $U_b(q)$ first. Now $U_b(r)$ includes: (a) The potential due to the nucleus and that due to the core electrons; (b) the potential arising from correlations among the core electrons; and (c) the potential due to exchange between core and conduction electrons.

These contributions have been evaluated by Loucks and Cutler[2] in their band-structure work. These authors define a quantity $h(r)$ related to the potential $V(r)$ (per ion) seen by an electron in the crystal by

$$h(r)=-rV(r)$$

and give in their Table II the contributions to $h(r)$ from various sources, including those mentioned above. The contributions (a), (b), and (c) required at present are available in columns 2, 3, and 4 of the table referred to. The potential $U_b(r)$ is therefore readily constructed, and $U_b(q)$ derived from it by performing the Fourier transform numerically.

Next we turn our attention to the repulsive part of the potential. Following Sham, we may define the average repulsive potential $\bar{U}_R(q)$ as

$$\bar{U}_R(q)=\left[\frac{1}{nN}\sum_{\mathbf{k}}\frac{n(\mathbf{k})-n(\mathbf{k}+\mathbf{q})}{E_{\mathbf{k}}-E_{\mathbf{k}+\mathbf{q}}}\right]^{-1} \times\left\{\frac{1}{nN}\sum_{\mathbf{k}}\frac{n(\mathbf{k})U_R(\mathbf{k},\mathbf{q})-n(\mathbf{k}+\mathbf{q})U_R^*(\mathbf{k}+\mathbf{q},-\mathbf{q})}{E_{\mathbf{k}}-E_{\mathbf{k}+\mathbf{q}}}\right\}. \tag{6}$$

Here N is the number of unit cells in the crystal and $n(\mathbf{k})$ is the occupation number of the state with wave vector $\mathbf{k}$. Further, $E_{\mathbf{k}}$ is the single-particle energy of the state $|\mathbf{k}\rangle$ and is taken to be the free-electron value. The summation over $\mathbf{k}$ includes also a sum over spin states of the electron. Further,

$$U_R(\mathbf{k},\mathbf{q})=nN\langle\mathbf{k}+\mathbf{q}|\,U_R\,|\mathbf{k}\rangle.$$

In other words, $(nN)^{-1}\,U_R(\mathbf{k},\mathbf{q})$ is the matrix element of the nonlocal operator U_R between plane-wave states $|\mathbf{k}\rangle$ and $|\mathbf{k}+\mathbf{q}\rangle$. From the above, it is clear that the problem of evaluating $\bar{U}_R(q)$ consists essentially in first determining $U_R(\mathbf{k},\mathbf{q})$ and then performing the average in (6). In the case of Be, these problems are, to some extent, simplified by the fact that the core has only $1s$ states.

For evaluating the matrix element and performing the subsequent averages, it is useful to have an analytical form for the core eigenfunctions. Loucks and Cutler have noted that the $1s$ function determined from their self-consistent calculations agreed very closely with the $1s$ function for neutral Be, as determined by Roothan, Sachs, and Weiss.[21] We have accordingly adopted the analytical form given by the latter authors, which is

$$\phi_{1s}(r)=\left(\frac{1}{4\pi}\right)^{1/2}\frac{P_{1s}(r)}{r},$$

where

$$P_{1s}(r)=\sum_{i=1}^{3}(A_i re^{-B_i r}+C_i r^2 e^{-B_i r}).$$

Here r is measured in atomic units and the quantities A_i, B_i, and C_i are constants and their values are listed in Table II. Using the above form for the core function, $U_R(\mathbf{k},\mathbf{q})$ becomes

$$U_R(\mathbf{k},\mathbf{q})=\frac{1}{\Omega_0}(E_{\mathbf{k}}-E_{1s})\int\phi_{1s}(r)e^{-i(\mathbf{q}+\mathbf{k})\cdot\mathbf{r}}d\mathbf{r} \times\int\phi_{1s}^*(r)e^{i\mathbf{k}\cdot\mathbf{r}}d\mathbf{r}$$
$$=\frac{4\pi}{\Omega_0}(E_{\mathbf{k}}-E_{1s})P_{1s}(\mathbf{k}+\mathbf{q})P_{1s}(\mathbf{k}),$$

where

$$P_{1s}(\mathbf{k})=\sum_{i=1}^{3}\left(\frac{2A_iB_i}{(B_i^2+\mathbf{k}^2)^2}+\frac{2C_i(3B_i^2-\mathbf{k}^2)}{(B_i^2+\mathbf{k}^2)^3}\right).$$

The expressions given above may now be used to compute $\bar{U}_R(q)$ from Eq. (6). In doing this we note that the curly bracket on the right-hand side of Eq. (6) may

TABLE II. Parameters occurring in the analytical form for $1s$ function.

i	A_i	B_i	C_i
1	2.94107	6.5	0.6088
2	11.72750	3.4	−0.55901
3	0.00784	0.9	−0.00195

[18] We follow Sham in ignoring the effects arising from the orthogonalization of plane waves to the core states.

[19] M. H. Cohen and V. Heine, Phys. Rev. **122**, 1821 (1961).

[20] B. J. Ausin, V. Heine, and L. J. Sham, Phys. Rev. **127**, 276 (1962).

[21] C. C. J. Roothan, L. M. Sachs, and A. W. Weiss, Rev. Mod Phys. **32**, 186 (1960).

be written as

$$\sum_{\mathbf{k}} \frac{n(\mathbf{k})\langle \mathbf{k}+\mathbf{q}|U_R|\mathbf{k}\rangle}{E_{\mathbf{k}}-E_{\mathbf{k}+\mathbf{q}}}+\sum_{\mathbf{k}} \frac{n(\mathbf{k})\langle \mathbf{k}-\mathbf{q}|U_R|\mathbf{k}\rangle^*}{E_{\mathbf{k}}-E_{\mathbf{k}-\mathbf{q}}}$$
$$=I+II \text{ (say)}.$$

On converting the summation into an integration and further choosing the Z axis along $\mathbf{q}$, the quantity I becomes

$$I=-\frac{2}{\pi}\int_0^{k_F}\int_0^{\pi} \frac{(k^2+6.765)P_{1s}(\mathbf{k})P_{1s}(\mathbf{k}+\mathbf{q})\sin\theta d\theta k^2 dk}{(q^2+2kq\cos\theta)},$$

where we have set $\hbar=1$, m (electron mass) $=\frac{1}{2}$, and expressed energy in rydbergs and wave vectors in inverse atomic units. The factor 2 comes from the spin summation and -6.765 is the $1s$ level energy (in rydbergs), as deduced by Loucks and Cutler (see Table I). The angular integration in the above expression is straightforward to perform though somewhat lengthy, and we shall merely give the final result. But before doing so we remark that II gives an identical result so that we eventually obtain

$$I+II=-\frac{4}{\pi}\int_0^{k_F}(k^2+6.765)P_{1s}(k)[X(k,q)/2q]kdk,$$

where

$$X(k,q)=\sum_{i=1}^{3}\left(-\frac{8A_iB_ikq}{a(k)b(k)c(k)}+\frac{2A_iB_id(k)}{[a(k)]^2}-\frac{32B_i^2C_i(B_i^2+k^2+q^2)kq}{a(k)[b(k)c(k)]^2}\right.$$
$$\left.-\frac{32B_i^2C_ikq}{[a(k)]^2b(k)c(k)}+\frac{8B_i^2C_id(k)}{[a(k)]^3}+\frac{8C_ikq}{a(k)b(k)c(k)}-\frac{2C_id(k)}{[a(k)]^2}\right),$$

the quanties $a(k)$, $b(k)$, $c(k)$, and $d(k)$ being defined as $a(k)=B_i^2+k^2$, $b(k)=B_i^2+(k+q)^2$, $c(k)=B_i^2+(k-q)^2$, and $d(k)=\ln[c(k)(q+2k)/b(k)]-\ln|q-2k|$.

The term in the square bracket on the right-hand side of Eq. (6) may be simplified as usual to yield the result

$$\frac{1}{nN}\sum_{\mathbf{k}}\frac{n(\mathbf{k})-n(\mathbf{k}+\mathbf{q})}{E_{\mathbf{k}}-E_{\mathbf{k}+\mathbf{q}}}=-\chi(q)Z,$$

so that we finally have

$$\bar{U}_R(q)=\frac{1}{\pi q\chi(q)}\int_0^{k_F}(k^2+6.765)P_{1s}(k)X(k,q)kdk.$$

The remaining integration, i.e., over k, is done numerically in a computer. It is interesting to compare the values of $\bar{U}_R(q)$ thus derived with those obtained for $U_R(k,q)$ when both $\mathbf{k}$ and $\mathbf{k}+\mathbf{q}$ are restricted to lie on the Fermi sphere. This is done in Fig. 1. For scatterings confined to the Fermi surface, we obtain a constant value since the core contains just $1s$ electrons. From the figure, we observe that there are fairly large differences between the two results unlike the case of Na,[17] where the difference did not exceed 3%. The screened pseudopotential

$$U^s(q)=[U_b(q)+\bar{U}_R(q)]/\epsilon(q),$$

derived using the procedure described above, and the dielectric function given in Eq. (5) is shown in Fig. 2. Using this pseudopotential, $E(q)$ was calculated upto a range of $(q/k_F)=12$ in steps ranging from 0.025 to 0.05 (in q/k_F), depending upon the local rate of variation of the function. Intermediate values, when required, were obtained through suitable polynomial interpolation. The electronic contribution to the dynamical matrix was obtained through the use of Eqs. (1) and (2) and the Coulombic contribution as mentioned earlier, and

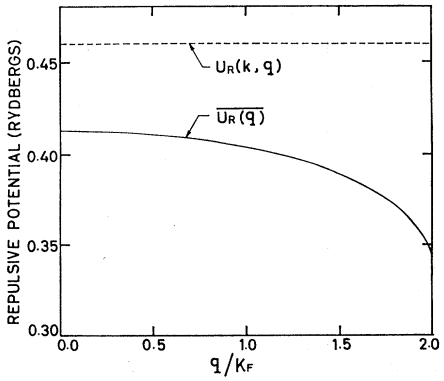

FIG. 1. Comparison of the average repulsive potential $\bar{U}_R(q)$ with $U_R(k,q)$, where $\mathbf{k}$ and $\mathbf{k}+\mathbf{q}$ both lie on the Fermi surface.

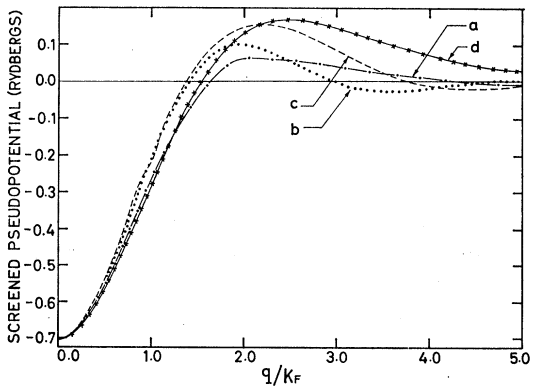

FIG. 2. Screened pseudopotential $U^s(q)$ for Be. The labels on the different curves indicate the following: (a) Derived from the results of Loucks and Cutler; (b) Animalu–Heine potential taken from Ref. 16 and suitably damped; (c) local model potential constructed by Animalu using the methods of Ref. 7; (d) potential derived from experimental phonon data.

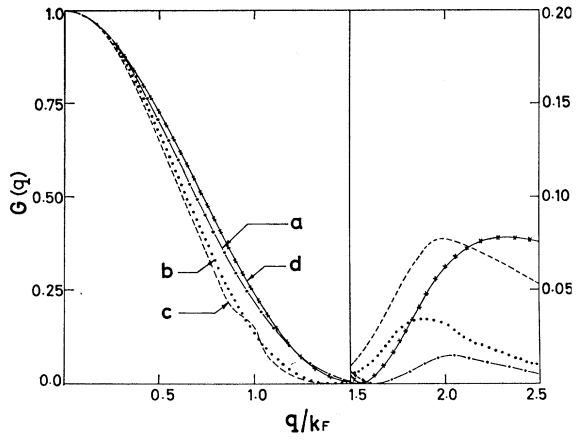

FIG. 3. $G(q)$ function for Be. The curves marked (a)–(d) are derived from the potentials with corresponding labels in Fig. 2.

the normal-mode frequencies computed in the usual manner. In calculating the electronic contribution, the summation in reciprocal space was extended over 900 reciprocal-lattice points to obtain satisfactory convergence.

In Fig. 3, we plot a quantity $G(q)$ which is related to $E(q)$ by[22]

$$G(q)=(-\tfrac{1}{2}4\pi Ze^2/q^2\Omega_0)^{-1}E(q).$$

This $G(q)$ function, [which incidentally is more convenient to plot than the $E(q)$ function] is the same as the $\phi(q)$ function of Sham[17] and of Animalu *et al.*[7] and the $G(q)$ function of Cochran.[23]

The results for the dispersion relations in the symmetry directions [0001] and [01$\bar{1}$0] are shown in Fig. 4 along with the experimental results of Schmunk *et al.*[3] The agreement between theory and experiment is of a qualitative nature only except for the transverse branches along the [0001] direction. These, however, are not much influenced by the behavior of the electrons.[1]

The poor agreement between theory and experiment is somewhat disappointing especially when we recall that the band-structure calculations on which our computations were based were performed very carefully.

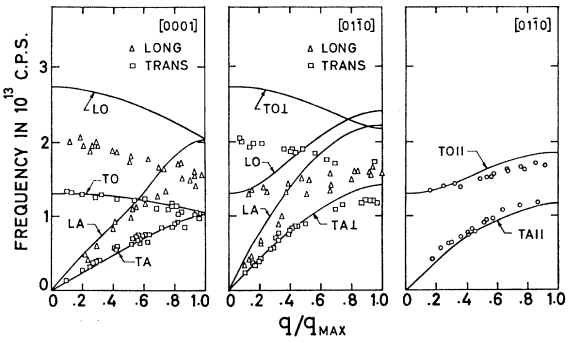

FIG. 4. Comparison of the theoretically computed dispersion relations based on basic pseudopotential with the experimental results of Schmunk *et al.*

It is pertinent at this juncture to comment briefly on a calculation made by Koppel and Young[24] along similar lines, and using the results of Loucks and Cutler. In our language, the potential entering Koppel and Young's work is

$$U(q)=U_b(q).$$

In other words, the repulsive part does not enter the formulation of these authors. Further, only the contributions (a) and (b) listed earlier are included in $U_b(q)$. The dielectric function used is same as in the present work. This calculation referred to in their paper as plane-wave approximation, yielded curves whose overall agreement was roughly of the same quality as in Fig. 4. We might also add that Koppel and Young carried out another calculation using a dielectric matrix based on a 23-OPW representation of the conduction-electron wave function. Unfortunately, this yielded poorer results than the plane-wave approximation.

III. CALCULATIONS BASED ON ANIMALU'S MODEL POTENTIAL

In this section, we shall consider the calculations based on the Animalu–Heine model potential.[5] This is an extension of the local model potential introduced earlier by Heine and Aberenkov,[25] and includes nonlocal effects. The screened model potential for Be is available in Harrison's book.[16] A notable feature of this potential is the rather long oscillatory tail which arises principally from a discontinuity in the model potential in real space. The oscillations have been damped as suggested by Animalu,[4] and the resulting potential is shown in Fig. 2 as curve b. The $G(q)$ function based on this potential has been computed by Animalu[4] and is shown as

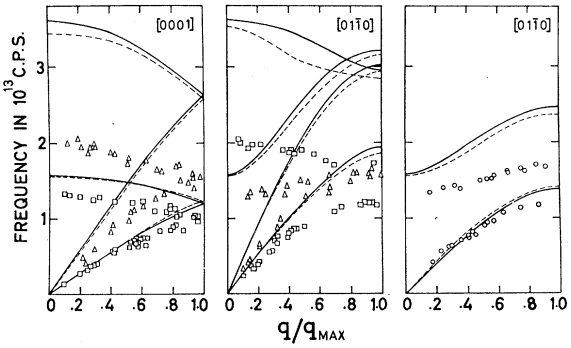

FIG. 5. Comparison of dispersion relations based on Animalu's model potentials with experiment. The solid line refers to potential (b) of Fig. 2, while the dashed line refers to potential (c) of the same figure.

[22] If the orthogonality effects are considered then the relationship between $G(q)$ and $E(q)$ is slightly different. See Ref. 4.

[23] W. Cochran, Proc. Roy. Soc. (London) **A276**, 308 (1963).

[24] J. U. Koppel and J. A. Young, in *Neutron Thermalization and Reactor Spectra* (International Atomic Energy Agency, Vienna, 1968), Vol. I, p. 333; see also J. U. Koppel and A. A. Maradudin, Phys. Letters **24A**, 224 (1967).

[25] V. Heine and I. Aberenkov, Phil. Mag. **9**, 451 (1964); **12**, 529 (1965).

curve b in Fig. 3. Animalu has also provided a tabulation of the $G(q)$ function in steps of 0.1 in (q/k_F). In our calculations, we require $G(q)$ at intermediate points and consequently we employed a polynomial interpolation scheme for that purpose. The dispersion relations obtained by us, using this $G(q)$, are presented in Fig. 5 as solid lines. In the calculation of the electronic contribution, it was found adequate to restrict the summation in reciprocal space to 233 points. This was possible on account of the more rapid decay of this $G(q)$ function at large q, as opposed to the one computed from first principles. To be consistent with Animalu, we employed the following lattice parameters used by him: $a=2.281$ Å, $(c/a)=1.5677$.[4] Turning to the figure, we observe that the agreement with experiment is generally worse than we had in Sec. II.

Recently, Animalu *et al.*[7] have had considerable success in predicting the dispersion relations for a number of cubic metals using a model potential which is similar to the Heine–Aberenkov potential, but avoids the difficulties associated with the discontinuity in real space referred to earlier. The screened model potential $U^s(q)$ computed using this procedure, and the $G(q)$ function based on it have kindly been provided to us by Animalu and they are displayed in Figs. 2 and 3 as curves c. The dispersion relations obtained using this $G(q)$ are shown as dashed lines in Fig. 5, and we find that the agreement with experiment has by no means improved.

The Heine–Animalu potential has also been employed by Brovman, Kagan, and Holas[26] for calculating the dispersion relations for Be. These authors believe that the lack of agreement with experiment is due to the presence of "nonpair" (i.e., noncentral) forces. Allowance for the extra contribution to the dynamical matrix arising from this source is made via the axially symmetric force-constant approach. The nonpair interactions are restricted to the two nearest-neighbor atoms, involving the use of three parameters whose values are adjusted by comparison with experiment. The agreement between theory and experiment is then considerably improved over that of Fig. 4, but at the expense, however, of three parameters.

The model potential scheme has also been employed by Gilat, Rizzi, and Cubiotti[27] recently to calculate the dispersion relations of the hcp metals Be, Mg, and Zn. These authors use the so-called optimum model potential,[28] which is an optimized variant of the Heine–Aberenkov–Animalu potential. The dispersion curves for Be calculated by Gilat *et al.* are very similar to those of Fig. 5 except perhaps that the upper branches are somewhat lower. For example, at the zone center, the longitudinal frequency computed by Gilat *et al.* is $\sim 3.15\times 10^{13}$ cps as opposed to the value of $\sim 3.6\times 10^{13}$ cps obtained in the present work.

IV. DERIVATION OF POTENTIAL FROM PHONON DATA

We consider finally the problem of deriving a potential from experimental data. This is usually done by assuming a suitable and physically plausible form for the (local) pseudopotential with a few adjustable parameters which are then determined by fitting to the experimental phonon data. The simplest among these is the one-parameter Bardeen potential.[29] One can, however, hardly get a good fit with just one parameter and so we shall not consider it any further. Next in the order of complexity comes the two-parameter model potential proposed by Harrison[30] and which was used in our earlier work on Mg. An extended version of such a potential involving more parameters has been used by Schneider and Stoll in their analyses of data for the alkali metals[31] and Mg.[8] The form of the potential used in this investigation is based on the Schneider and Stoll expression, and is given by

$$U(q)=-\frac{4\pi Ze^2}{q^2\Omega_0}+\frac{\beta_1}{[1+(qr_1)^2]^2}+\frac{\beta_2(qr_2)^2}{[1+(qr_2)^2]^4}, \quad (7)$$

where β_1, β_2, r_1, and r_2 are adjustable parameters. Z is the valency of the ion and Ω_0 the atomic volume.

With this form for the pseudopotential, we have a nonlinear least-squares problem which is solved by a standard technique. The method consists in starting with some trial values for the parameters[32] and using these, the pseudopotential and phonon frequencies are computed. These frequencies are compared with the experimental frequencies, and increments to the various parameters are determined so as to minimize the variance. The increments are then added to the parameters and the cycle repeated till the process converges. In our present work, convergence was obtained after four cycles of refinement. As there is considerable scatter in the data of Schmunk *et al.* we have for the purpose of fitting, taken a smooth line through the experimental points as giving the experimental frequencies. The final parameters derived by fitting are given in Table III. The corresponding screened pseudopotential and $G(q)$

TABLE III. Pseudopotential parameters for Be derived from fitting to experimental phonon data.

r_1	0.883 a.u.
r_2	0.298 a.u.
β_1	0.331 Ry
β_2	3.270 Ry

[26] E. G. Brovman, Yu. Kagan, and A. Holas, in *Neutron Inelastic Scattering* (International Atomic Energy Agency, Vienna, 1968), Vol. I, p. 165.

[27] G. Gilat, G. Rizzi, and G. Cubiotti, Phys. Rev. (to be published). We are grateful to Dr. Gilat for communicating these results prior to publication.

[28] R. W. Shaw, Jr., Phys. Rev. **174**, 769 (1968).

[29] L. J. Sham and J. Ziman, in *Solid State Physics*, edited by F. Seitz and D. Turnbull (Academic Press Inc., New York, 1963), Vol. 15, p. 221.

[30] W. Harrison, Phys. Rev. **139**, A179 (1965).

[31] T. Schneider and E. Stoll, Physik Kondensierten Materie **5**, 331 (1966).

[32] These are deduced in a manner somewhat similar to that employed in Ref. 1.

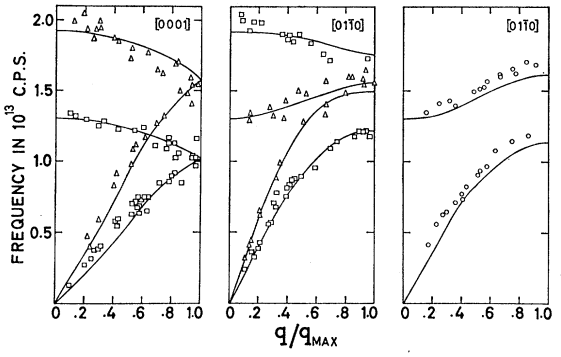

FIG. 6. Fit achieved to the experimental phonon dispersion relations using a potential of the form given in Eq. (7) with the values of the parameters as in Table III.

function are shown respectively in Figs. 2 and 3 as curve d, while the fit achieved is indicated in Fig. 6.

Mention may also be made of the fit to experiment made by Brovman, Kagan, and Holas.[26] These authors use a two-parameter local model potential together with a three-parameter noncentral interaction. The total number of parameters is thus five and the over-all fit is of about the same quality as in Fig. 6. It is interesting to note that the model potential of Brovman *et al.* resembles closely the potential d of our Fig. 2, especially in the strong tail beyond the first intersection of $U^s(q)$ with the q axis.

The pseudopotential derived from experimental phonon data should hopefully be useful in computing the various other properties of Be, particularly the electronic properties. By way of examining the utility of this potential, we have carried out a band-structure calculation and also determined representative dimensions of the Fermi surface. The band-structure calculations were performed as follows: Now as is well known, the conduction-electron energies E_k in rydbergs may be obtained from the coupled equations[16]

$$\sum_j \Big([(\mathbf{k}+\tau_j)^2 - E_k]\delta_{jj'} + U^s(|\tau_{j'}-\tau_j|) - \frac{1}{n} \times \sum_k e^{-i(\tau_{j'}-\tau_j)\cdot r(k)} \Big) C_j = 0. \quad (8)$$

In this equation, C_j is one of the coefficients occurring in the expansion of the "pseudo-wave-function" in terms of the plane waves $|\mathbf{k}+\tau_j\rangle$, and $(\mathbf{k}+\tau_j)^2$ is the diagonal matrix element

$$\langle \mathbf{k}+\tau_j | T | \mathbf{k}+\tau_j \rangle$$

of the kinetic-energy operator T. In principle, the summation over j in the second term on the left-hand side of Eq. (8) extends over the whole of reciprocal space, but in practice it is restricted to a few terms, leading thereby to a truncated secular determinant. In our calculations, we have included the 14 reciprocal-lattice vectors nearest to the vector $\mathbf{k}$ in the Brillouin zone, and the energy eigenvalues were obtained by diagonalizing the resulting 14-dimensional matrix. The band-structure results thus obtained are displayed in part (iii) of Fig. 7. Also shown for purposes of comparison are the

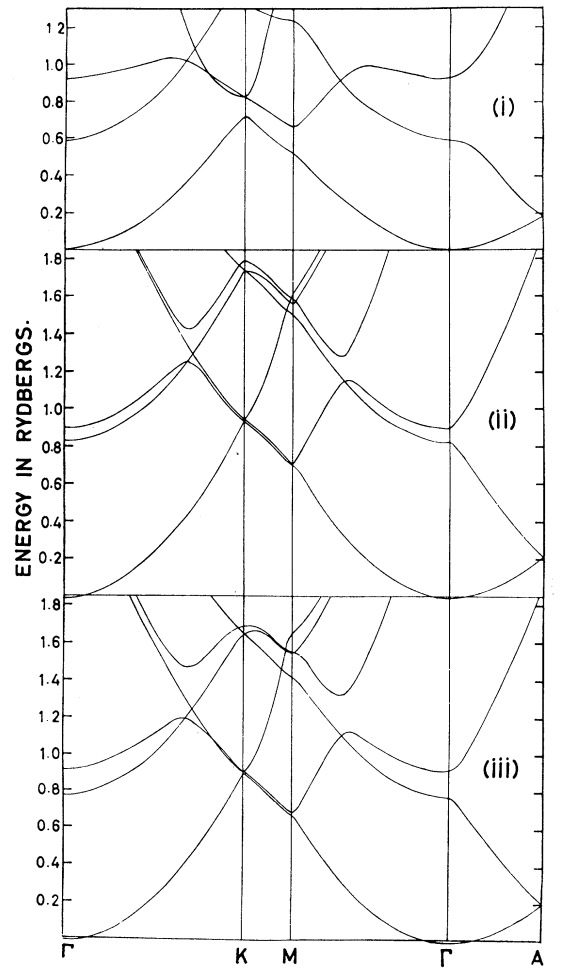

FIG. 7. Band-structure results for Be. (i) OPW results of Loucks and Cutler; (ii) based on basic pseudopotential; (iii) based on fitted pseudopotential.

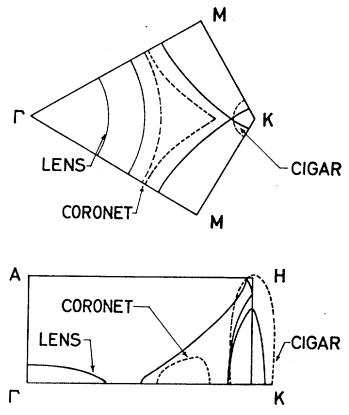

FIG. 8. Representative sections of the Fermi surface of Be. The solid lines are the results of present calculation while the dashed lines are those obtained by Watts (Ref. 10) from experiment.

OPW results of Loucks and Cutler [part (i)] and the band structure based on the basic pseudopotential [part (ii)]. A noteworthy feature of these results is that both pseudopotentials yield very nearly free-electron-like band structures as compared to the OPW calculations. As remarked earlier, the same result was also found with the model potentials of Animalu.

The Fermi energy based on the band structure of Fig. 7(iii) was calculated along the lines of Ref. 2 and found to be 1.023 Ry. Representative sections of the Fermi surface based on this potential and the above value of E_F are shown as solid lines in Fig. 8. The dashed lines in the figure show the corresponding sections as deduced from experiment by Watts.[10] As can be seen, the agreement between the computed and measured Fermi surface is rather poor. In particular, the lens in the third band is not seen in experiment. This lack of agreement is in marked contrast to the situation in Mg for which Stoll and Schneider[8] find that the fitted pseudopotential is able to give a fairly good account of the measured Fermi surface which, it must be pointed out, is more nearly free-electron-like than that of Be. It would appear, therefore, that unlike in the case of Mg, it is not possible to obtain a unified description of the properties of Be using the same (empirical) pseudopotential.

PHYSICAL REVIEW VOLUME 185, NUMBER 3 15 SEPTEMBER 1969

Low-Field Hall Coefficient of Indium†

JAMES C. GARLAND
Laboratory of Atomic and Solid State Physics, Cornell University, Ithaca, New York 14850
(Received 24 March 1969)

This paper reports measurements of the magnetic field and temperature dependence of the Hall coefficient of both single-crystal and polycrystalline indium in the regime characterized by $\omega_c\tau<1$. Measurements were performed at temperatures below 4.5°K using the helicon-wave technique. The normally positive Hall coefficient was observed to reverse sign at fields below a few hundred gauss with the field **H** oriented along the [100] and [111] crystal axes. The magnitude of the "crossing field" H_0 as well as the zero-field coefficient $R(0)$ was observed to decrease with increasing temperature. We have analyzed our results in terms of a two-band model of the Hall coefficient and have concluded that the ratio of the electron relaxation time to the hole relaxation time is less than unity and decreases with increasing temperature.

I. INTRODUCTION

THE Fermi surface of indium is thought to consist of a large second-zone hole surface comprising about 99% of the total number of carriers, and a small third-zone electron surface which makes up the remainder.[1] At high fields, the traditional theory of the Hall effect maintains that the Hall coefficient R should be independent of magnetic field, and should reflect only the relative carrier densities of the two types of carriers, i.e.,

$$R=1/ec(n_1-n_2)\,, \tag{1}$$

where n_1 represents the hole density and n_2 the electron density. Thus, at high fields the Hall coefficient of indium is positive, with a value of 1.6×10^{-13} V cm/A Oe, corresponding to about 1.01 holes per atom and to 0.01 electrons per atom. At lower fields, however, when $\omega_c\tau$ is comparable to or less than unity for at least one group of carriers, the Hall coefficient is not only field-dependent but also depends sensitively on the scattering times and effective masses of the holes and electrons. If we write $R_1=1/n_1ec$, $R_2=1/n_2ec$, and let σ_1 and σ_2 represent the conductivities of the hole and electron bands separately, then the two-band Hall coefficient is given by[2]

$$R(H)=\frac{\sigma_1^2R_1-\sigma_2^2R_2+H^2\sigma_1^2\sigma_2^2R_1R_2(R_2-R_1)}{(\sigma_1+\sigma_2)^2+H^2\sigma_1^2\sigma_2^2(R_1-R_2)^2}. \tag{2}$$

In the high-field limit this is seen immediately to reduce to Eq. (1), while for $H=0$ we obtain (after writing $\sigma_1=n_ie^2\tau_i/m_i^*$)

$$R(0)=-\frac{1}{ec}\frac{(\tau_1/m_1^*)^2n_1-(\tau_2/m_2^*)^2n_2}{(n_1\tau_1/m_1^*+n_2\tau_2/m_2^*)^2}. \tag{3}$$

Although the applicability of Eq. (3) is limited to very simple metals, it is reasonable to expect a more general expression for $R(0)$ to vary with crystal orientation and to reflect the anisotropy of the carrier effective masses. Furthermore, we have no guarantee that τ_1 and τ_2 are the same for each band or that they are orientation-independent, even though this is an assumption that is customarily made. There is at present very little experimental information on the anisotropy of scattering times in metals, particularly on the differences in scattering

† Work supported by the U. S. Atomic Energy Commission, under Contract No. AT(30-1)-2150, Technical Report No. NYO-2150-52, and the Advanced Research Projects Agency through the Materials Science Center at Cornell University, MSC Report No. 1136.

[1] N. W. Ashcroft and W. E. Lawrence, Phys. Rev. 175, 938 (1968).

[2] A. H. Wilson, *The Theory of Metals* (Cambridge University Press, Cambridge, England, 1958).